

Light Adaptation in Retinal Rods of the Rabbit and Two Other Nonprimate Mammals

K. NAKATANI, T. TAMURA, and K.-W. YAU

From the Howard Hughes Medical Institute and Department of Neuroscience, The Johns Hopkins University School of Medicine, Baltimore, Maryland 21205

ABSTRACT The responses of rabbit rods to light were studied by drawing a single rod outer segment projecting from a small piece of retina into a glass pipette to record membrane current. The bath solution around the cells was maintained at near 40°C. Light flashes evoked transient outward currents that saturated at up to ~20 pA. One absorbed photon produced a response of ~0.8 pA at peak. At the rising phase of the flash response, the relation between response amplitude and flash intensity (I_f) had the exponential form $1 - e^{-k_f I_f}$ (where k_f is a constant denoting sensitivity) expected from the absence of light adaptation. At the response peak, however, the amplitude–intensity relation fell slightly below the exponential form. At times after the response peak, the deviation was progressively more substantial. Light steps evoked responses that rose to a transient peak and rapidly relaxed to a lower plateau level. The response–intensity relation again indicated that light adaptation was insignificant at the early rising phase of the response, but became progressively more prominent at the transient peak and the steady plateau of the response. Incremental flashes superposed on a steady light of increasing intensity evoked responses that had a progressively shorter time-to-peak and faster relaxation, another sign of light adaptation. The flash sensitivity changed according to the Weber–Fechner relation (i.e., inversely) with background light intensity. We conclude that rabbit rods adapt to light in a manner similar to rods in cold-blooded vertebrates. Similar observations were made on cattle and rat rods.

INTRODUCTION

The retinal rods of almost every cold-blooded vertebrate species that has been studied are found to adapt to light (Dowling and Ripps, 1972; Baylor and Hodgkin, 1974; Coles and Yamane, 1975; Kleinschmidt and Dowling, 1975; Fain, 1976; Hemilä, 1977; Baylor et al., 1979a, 1980; Lamb et al., 1981; Copenhagen and Green, 1985; Leibovic et al., 1987). This adaptation property can be recognized in one or

Address reprint requests to Dr. K.-W. Yau, Department of Neuroscience, The Johns Hopkins University School of Medicine, 725 N. Wolfe Street, Baltimore, MD 21205.

Dr. Tamura's present address is Department of Ophthalmology, Kanazawa University School of Medicine, 13-1 Takara-machi, Kanazawa, Ishikawa 920, Japan.

more ways. First, the time-to-peak of the rod response to a flash becomes progressively shorter with increasing flash intensity, suggesting the growing influence of an adapting process at higher light intensities (see, for example, Baylor et al., 1979a). Second, the response of a rod to a step of light typically rises to a transient peak but then relaxes to a lower steady level, again indicative of the progressive development of an adapted state of the cell, in which the effect of an absorbed photon is reduced (see, for example, Baylor and Hodgkin, 1974; Coles and Yamane, 1975; Kleinschmidt and Dowling, 1975; Fain, 1976; Baylor et al., 1979b, 1980). Finally, the reduction in flash sensitivity caused by background light obeys the Weber–Fechner relation, quantitatively expressed as an inverse relation between incremental flash sensitivity and background light intensity (for review, see Shapley and Enroth-Cugell, 1984); at the same time, the time course of the flash response is shortened by the background light (Baylor and Hodgkin, 1974; Kleinschmidt and Dowling, 1975; Baylor et al., 1979a, 1980). The underlying mechanism for this adaptation is now known to involve a Ca^{2+} -mediated negative feedback regulation in the phototransduction process (Yau and Nakatani, 1985; Koch and Stryer, 1988; Matthews et al., 1988; Nakatani and Yau, 1988a; see also Gold, 1986; Korenbrot and Miller, 1986; McNaughton et al., 1986; Torre et al., 1986; Yau et al., 1986; Miller and Korenbrot, 1987; Hodgkin and Nunn, 1988; Nakatani and Yau, 1988b; Ratto et al., 1988; Rispoli et al., 1988; Kawamura and Murakami, 1989; Nakatani and Yau, 1989b; for review, see Yau and Baylor, 1989).

A few years ago it was reported that macaque monkey rods behave quite differently, in that the above characteristics of adaptation are scarcely observed in these cells (Baylor et al., 1984). This raises the possibility of a basic difference between mammalian rods and those of lower vertebrates, and perhaps more generally between rods in warm-blooded and in cold-blooded animals (see, for example, Pugh and Altman, 1988). To examine this question more closely, we have recorded from rods of a variety of mammals, and have found, quite surprisingly, that all of these cells show clear signs of light adaptation. The experiments on cat rods have briefly been reported elsewhere (Tamura et al., 1989). In this paper we describe in greater detail the experiments on rabbit rods; experiments on cattle and rat rods are also included to provide a broader survey of mammalian species.

Preliminary results from the experiments on rabbit rods have appeared (Nakatani and Yau, 1989a).

METHODS

Rabbit Experiments

Animals and retinal preparation. The albino rabbit was used in all of the experiments. The animals were kept in the animal quarters of the Division of Comparative Medicine at Johns Hopkins School of Medicine. An animal was dark-adapted for an hour or longer immediately before use. In the early experiments the animal was killed by decapitation, and one or both eyes were then removed in dim red light. In later experiments the animal was put under general anesthesia with sodium pentobarbital, then killed by an intravenous overdose of pentobarbital after removal of the eyes. All subsequent procedures were performed under infrared light. An eye was coronally hemisected and, under Locke solution (see below), several small pieces of peripheral retina were removed from the posterior eyecup. The retinal pieces

were kept in oxygenated DMEM or L-15 culture medium (Gibco Laboratories, Grand Island, NY) in a light-tight container in the refrigerator, and used over a period of up to 12 h. When needed, a piece of retina was washed twice in Locke solution, then placed receptor-side up on cured Sylgard in a small petri dish containing the same solution and chopped finely with a razor blade. The chopped retinal pieces were transferred into the experimental chamber with a micropipette. In some later experiments the retina was also treated before chopping with purified collagenase (CLSPA grade; Worthington Biochemical Corp., Freehold, NJ) at 0.3 mg/ml to remove extracellular matrix (see Baylor et al., 1984); this step made sucking a rod outer segment into the recording pipette easier. The experimental findings were the same with and without enzyme treatment.

Recording and light stimulation. Details of the recording method and the experimental chamber are described in Baylor et al. (1979a), Lamb et al. (1981), and Hodgkin et al. (1984). Briefly, membrane current was recorded from a single rod outer segment projecting from a fragment of retina by sucking it into a glass pipette that contained Locke solution and was connected to a current-to-voltage converter. The position of the rod outer segment was adjusted so that the ciliary connection between the outer and the inner segments was situated at the constriction of the pipette tip. Manipulations were made with the help of an infrared-sensitive TV camera system attached to the microscope. The pipette was coated with silane and had a tip inner diameter of $\sim 1.5 \mu\text{m}$, chosen to provide a snug fit around the rabbit rod outer segment. When filled with Locke solution, it had a typical resistance of 3–5 M Ω when empty and 10–15 M Ω with an outer segment in place. Assuming that the resistance of the empty electrode was equally distributed between its very tip and the shank, we calculated that $\sim 80\%$ of the membrane current at the rod outer segment should be recorded. No corrections have been made for this incomplete current collection. In all of the figures, outward membrane current at the outer segment is plotted upwards. All records were stored on tape during the experiment and subsequently digitized on a computer and plotted. The traces shown in the figures have been low-pass filtered, with the high frequency cutoff set at 25–100 Hz.

The optical bench design was also similar to that described in Baylor et al. (1979a) and Lamb et al. (1981). Diffuse, unpolarized light at 500 nm was used in all experiments, with the light incidence being approximately perpendicular to the longitudinal axis of the recorded outer segment. When light flashes were used, they were all ~ 8 ms in duration. The recorded rod outer segments had, on average, a diameter of $\sim 1.5 \mu\text{m}$ and a length of $\sim 15 \mu\text{m}$. Assuming an optical density of $0.016 \mu\text{m}^{-1}$ (Liebman, 1972; Harosi, 1975) and a quantum efficiency of 0.67 (Dartnall, 1972), an effective collecting area of $0.35 \mu\text{m}^2$ under our experimental conditions can be calculated (see Baylor et al., 1979b). Dr. Robert E. Marc of the University of Texas Medical Center at Houston kindly measured for us the dimensions of rod outer segments in fixed specimens of peripheral rabbit retina, and arrived at an average length of $\sim 20 \mu\text{m}$. Thus, some of the rod outer segments we experimented with possibly had their tips broken off; alternatively, our experimental procedure could have selected for cells with short outer segments, which were more likely to be spared during the chopping of the retina.

Solutions and temperature control. The Locke solution (see Baylor et al., 1984) contained (in mM): 140 NaCl, 3.6 KCl, 1.2 CaCl₂, 2.4 MgCl₂, 3 Na-HEPES, 10 dextrose, and 0.02 Na-EDTA, pH 7.6. The bath solution was heated by a glass-shielded platinum wire connected to a stabilized DC power supply. The temperature near the rod outer segment was measured by a thermistor probe (Yellow Springs Instrument Co., Yellow Springs, OH) attached to the suction pipette, with the sensor of the probe situated within 0.5 mm behind the tip of the pipette (see Baylor et al., 1980). The temperature was maintained as close as possible to 40°C, the body temperature of the rabbit, and was generally in the range of 38–41°C. In order to maintain the constancy of temperature, no perfusion was used during the run of an experiment.

Experiments on Cattle and Rat

Similar experiments were performed on rods from cattle and the albino rat. The bovine eyes were obtained from the local abattoir and transported back to the laboratory in ice-cold Locke solution (same composition as for rabbit) in a dark container to be dissected ~30 min later. The rat was dark-adapted overnight and killed by decapitation, followed by pithing of the brain. All other procedures were identical to those described above for the rabbit, except that the retina was treated with 0.3 mg/ml hyaluronidase (type IV; Sigma Chemical Co., St. Louis, MO) together with collagenase in some of the experiments. During experiments, the temperature in the vicinity of the pipette tip was maintained at 38–40°C. In a few experiments the experimental chamber was continuously perfused with preheated Locke solution, instead of a heating wire, to offset any water evaporation. There was no difference in observations with this alternative method.

The outer segments of the cattle rods were on average 18 μm long and 1.5 μm in diameter. The rat rod outer segments were ~15 μm long and 1.2 μm in diameter. In both cases, the diameters were only rough estimates because of their smallness.

RESULTS

Rabbit

Responses to flashes. Fig. 1 shows a family of responses of a rabbit rod to flashes of increasing intensity. The traces, especially those for dim flashes, represent averages of many trials. The saturated response amplitude for this cell was ~15 pA. From seven rods, the saturated current ranged from 10.5 to 17 pA (mean \pm SD = 13.3 ± 2.6 pA). From the dimmest flash intensity and the corresponding response, it was calculated that one absorbed photon should produce a peak outward current of ~0.7 pA (± 0.1 pA, SD). This single-photon response amplitude can also be estimated, without involving light calibrations and estimates of the effective collecting areas of the outer segments, simply from the ratio σ^2/m , where σ^2 is the variance and m is the mean of the response peak amplitude produced by repeated, identical dim flashes (see Baylor et al., 1979b). From the seven rods, this ratio was 0.8 pA (± 0.4 pA, SD). The absolute flash sensitivity measured here is fairly similar to those previously found in rat and primate rods (Penn and Hagins, 1972; Baylor et al., 1984). However, the saturated photocurrent (which represents the magnitude of the dark current; see Baylor et al., 1979a) is on average smaller when compared with these other species. It is possible that some of the rods we used had lost a fraction of their dark current by having the tips of their outer segments broken off (see Methods). However, the fact that the amplitude of the single-photon response in these rods remained large would suggest that their outer segments probably sealed off, with an undiminished dark current density through the rest of the outer segment.

The response to the dimmest flash in Fig. 1 reached peak in ~155 ms. The responses to brighter flashes reached peak progressively earlier, as indicated by the dashed line, which essentially intersects the peaks of all nonsaturating responses. From five rods in which we obtained a complete family of responses at different flash intensities, the fractional reduction in the response time-to-peak from the dimmest to the just-below-saturating light stimuli was, on average, 29% ($\pm 8\%$, SD). This relative shift is close to that previously observed in amphibian rods (~30% if averaged from

Fig. 3 of Baylor et al., 1979a, Fig. 1 of Baylor et al., 1984, and Fig. 3 of Baylor and Nunn, 1986).

The dependence of the response time-to-peak on flash intensity, though not very steep, suggests the existence of light adaptation in rabbit rods. More convincing evidence, however, came from an analysis of the relation between response amplitude and flash intensity. Fig. 2A shows this relation, in normalized form, for the experiment of Fig. 1 at three different time instants on the rising phase of the responses (50, 70, and 90 ms after the flash, respectively). The smooth curves all have

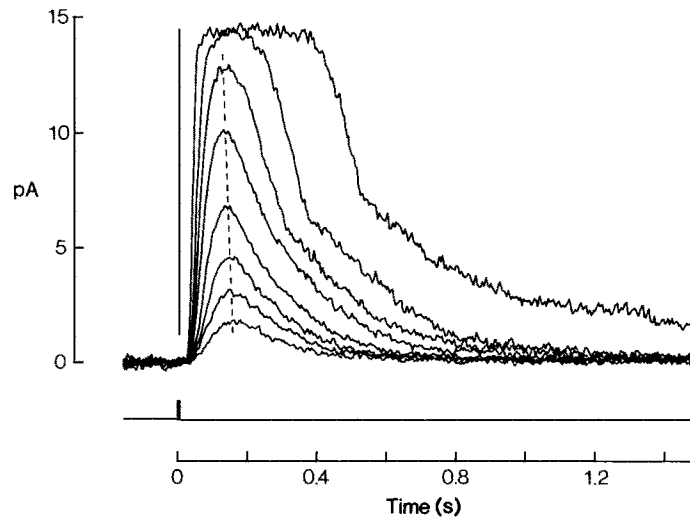


FIGURE 1. Family of flash responses elicited from a rabbit rod. Timing of flash (8 ms in duration) is indicated below the responses. Dashed line intersects approximately the peaks of all subsaturation responses; its slant indicates the progressive shortening of response time-to-peak with increasing flash intensity. Flash intensities were 7.6, 14, 28, 55, 1.1×10^2 , 2.1×10^2 , 4.1×10^2 , and 1.6×10^3 photons μm^{-2} , respectively; the corresponding responses were averages of 16, 10, 11, 10, 7, 5, 4, and 2 trials. Bandwidth was DC-100 Hz. Temperature was 41°C.

the same form, but are simply shifted on the abscissa to coincide with the respective sets of points. They are drawn according to:

$$\hat{r}_F = 1 - e^{-k_F I_F} \quad (1)$$

where \hat{r}_F is the normalized flash response amplitude, I_F is the flash intensity, and k_F is a proportionality constant denoting a cell's sensitivity to light. This relation describes an overall response of the cell that is composed of a statistical superposition of invariant (i.e., nonadapting) single-photon responses, each of which corresponds to a regional, complete closure of the light-regulated conductance (Lamb et al., 1981; Baylor et al., 1984). In other words, the curves show the expected response-intensity relation if there were no light adaptation. At least up to 90 ms after the flash (filled circles), this condition seemed to be roughly fulfilled.

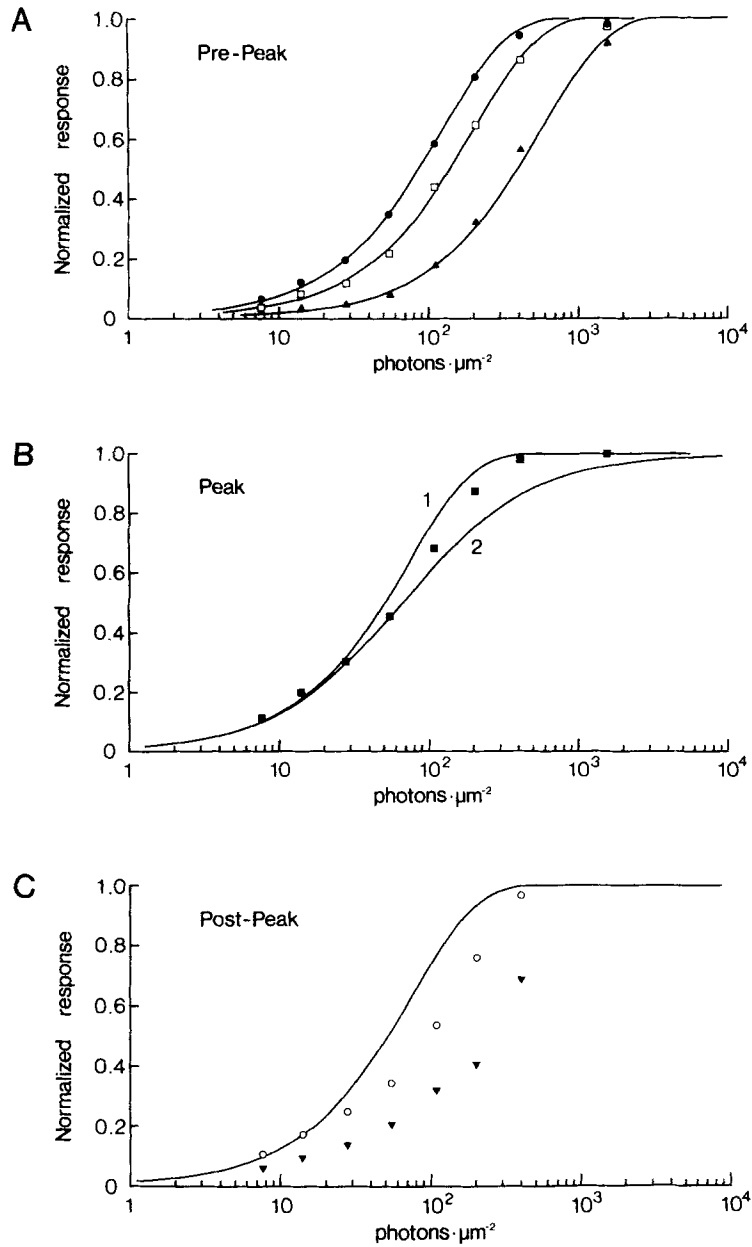


FIGURE 2. Response-intensity relations derived from the flash response family of Fig. 1. (A) Instantaneous relation measured at 50 ms (\blacktriangle), 70 ms (\square), and 90 ms (\bullet) after the flash. (B) Relation measured at response peak. (C) Instantaneous relation measured at 200 ms (\circ) and 300 ms (\blacktriangledown) after the flash. Curve 1 in B and all curves in A and C are drawn according to Eq. 1. Curve 2 in B is drawn according to Eq. 2.

Fig. 2 *B* shows the response–intensity relation at the response peak (which, of course, does not really correspond to a fixed time after the flash, because the response time-to-peak became slightly shorter with increasing flash intensity). Curve 1 is again drawn from Eq. 1. In this case, there is a conspicuous deviation of the experimental points from the curve, suggesting that some adaptation was already present. For comparison, curve 2 is drawn according to the more familiar Michaelis (or hyperbolic) relation describing response saturation, given by:

$$\hat{r}_F = \frac{I_F}{I_F + \sigma_F} \quad (2)$$

where σ_F is the half-saturating flash intensity. Clearly the points are intermediate between the two curves. In amphibian rods, the observed response–intensity relation at response peak also deviates from the Michaelis relation in the manner shown here, though perhaps to a lesser degree (Baylor et al., 1979*a*).

Fig. 2 *C* shows the response–intensity relation measured at two time instants after the response peak (200 and 300 ms after the flash, respectively). Deviation from Eq. 1 (continuous curve) is much more pronounced in these cases. From the trend indicated by the triangles, it is obvious that the relation at 300 ms after the flash falls even below the Michaelis relation. Thus, light adaptation develops further after the peak of the response. In general, an intensity–response relation measured at a time instant after the flash response peak, such as those shown in Fig. 2 *C*, can be particularly effective in diagnosing light adaptation that develops only slowly after a flash.

Fig. 3 shows collected results from the five rabbit rods, with essentially the same conclusion. In both panels, the relations obtained from different cells are compared by first fitting the foot of each experimental relation to the theoretical curves before plotting on a normalized abscissa. In *A*, curves 1 and 2 are from Eqs. 1 and 2, respectively. In *B*, the experimental relations were measured at 200 ms after the flash.

Responses to light steps. Fig. 4 shows the responses of the same rod as in Fig. 1 to steps of light at different intensities. The low frequency noise in the traces was due to photon fluctuations. One prominent feature shown by the responses at brighter intensities is the relaxation from an initial peak, again a sign of light adaptation. Fig. 5 *A* shows the response–intensity relation obtained from this experiment at several time instants on the rising phase of the responses (50, 60, 70, and 90 ms after the beginning of the light step), and Fig. 5 *B* shows the relation measured at the transient peak as well as at the plateau level near the end of the light step. The smooth curves in both panels are again drawn according to the exponential relation denoting no adaptation:

$$\hat{r}_S = 1 - e^{-k_S I_S} \quad (3)$$

where in this case \hat{r}_S is the normalized step response, I_S is the step intensity, and k_S is a proportionality constant. As in the flash experiments, the experimental relations at the rising phase of the responses showed little or no sign of light adaptation; the mild deviations of the relations at 70 and 90 ms from the smooth curves could be real, or could have resulted from photon fluctuations not completely removed by the very

limited trial-averaging. The relations at the transient peak and the steady state, on the other hand, clearly give strong indications of the presence of light adaptation. In Fig. 5 *B*, the position of the curve is constrained by the relation $k_s = k_F \cdot t_i$, where t_i is the integration time of the dim flash response from the same cell, and k_F is the sensitivity constant in Eq. 1 evaluated by fitting this equation to the foot of the response–intensity relation at response peak (see Fig. 2 *B*) (Baylor et al., 1984; Nakatani and Yau, 1988a; Tamura et al., 1989). This calculated position shows what

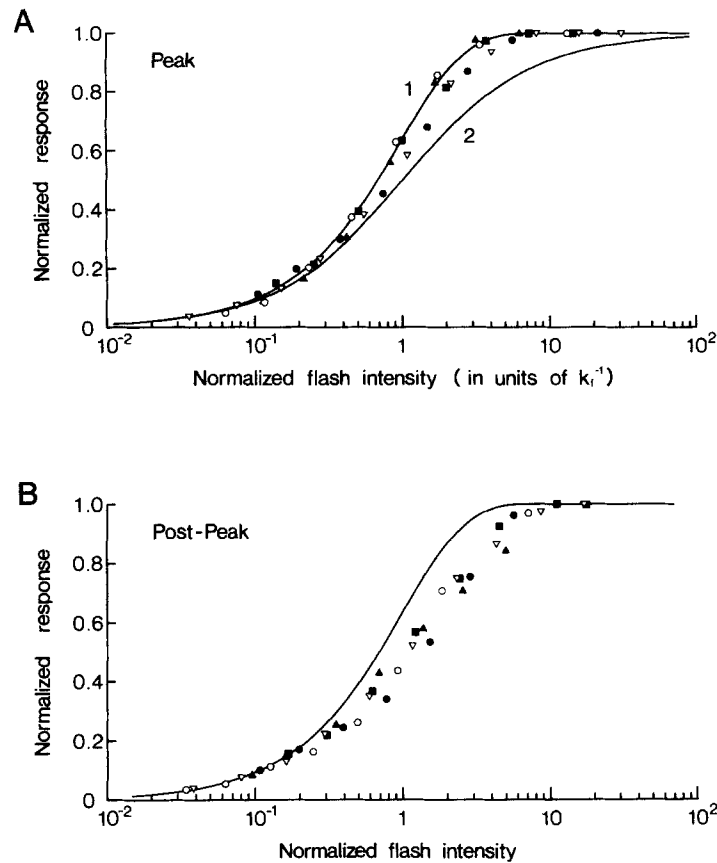


FIGURE 3. Collected flash response–intensity relations from five rabbit rods, plotted on normalized axes (see text). (A) Relation at response peak. (B) Instantaneous relation at 200 ms after the flash. Curve in B and curve 1 in A are drawn from Eq. 1. Curve 2 is drawn from Eq. 2. Temperature was 39–41°C. Saturated photocurrent was 11–17 pA.

would be expected in steady state if the single-photon responses were nonadapting and summated statistically. The curve coincides reasonably well with the experimental points at the lowest two light intensities, where interactions among individual photon effects should be minimal. The deviation between prediction and data, however, rapidly increases at higher intensities, where the effects of individual photons should interact much more in space and time along the outer segment.

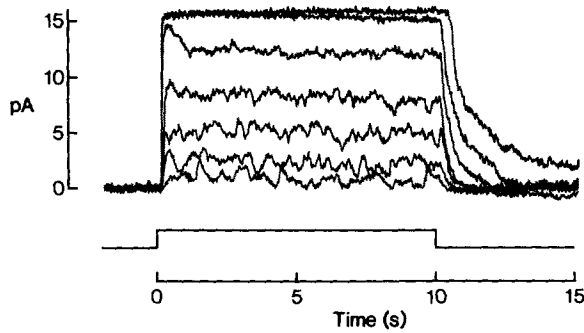


FIGURE 4. Family of responses to light steps elicited from a rabbit rod. Same cell as in Fig. 1. Timing of light step (10 s) is indicated below the responses. Light intensities were 13, 46, 1.7×10^2 , 5.9×10^2 , 2.3×10^3 , 8.3×10^3 , and 3.3×10^4 photons $\mu\text{m}^{-2} \text{s}^{-1}$, respectively; the corresponding responses were averages of 2, 2, 2, 2, 1, and 1 trials. Band-

width was DC-25 Hz. Temperature was 38°C (different from Fig. 1 because of progressive drift during the experiment).

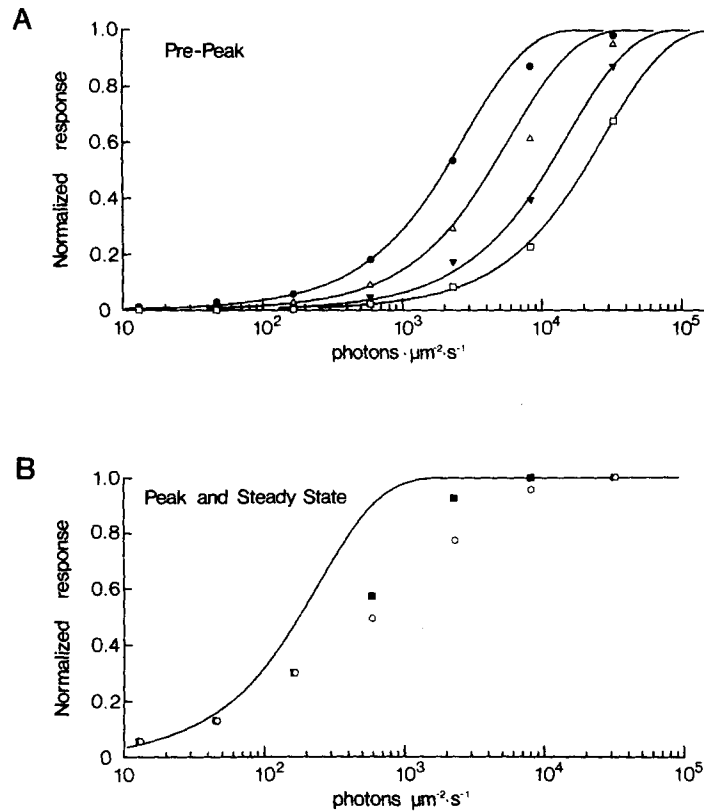


FIGURE 5. Response-intensity relations derived from the step response family of Fig. 4. (A) Instantaneous relation measured at 50 ms (\square), 60 ms (\blacktriangledown), 70 ms (\triangle), and 90 ms (\bullet) after the beginning of the light step. (B) Relation measured at transient response peak (\blacksquare) and steady state (\circ). For the next-to-brightest light step, the "steady-state" response is defined as the amplitude level attained just before the turning off of the light step. Curves in A and B are all drawn according to Eq. 3. In order to resolve the response amplitudes at early times after the turning on of the light step, the rising phase of the responses in Fig. 4 was redigitized with a bandwidth of DC-200 Hz.

Fig. 6 shows the responses to steps of light from another rod that had the most prominent relaxations observed. This cell is atypical, but it underscores the point that a mammalian rod can show even more pronounced adaptation than amphibian rods (cf., for example, Baylor et al., 1979b, 1980). Fig. 7 shows collected results from six rods, plotted on normalized coordinates. In Fig. 7 B, the relative position between the smooth curve and the experimental points for each cell is again constrained by the relation $k_s = k_F \cdot t_i$ as described above. On average, the steady-state step response reached half-saturation at ~ 500 photons $\mu\text{m}^{-2} \text{s}^{-1}$, and saturated at slightly over 10^4 photons $\mu\text{m}^{-2} \text{s}^{-1}$. These values are converted to photoisomerizations second^{-1} in Table I.

Reduction of flash sensitivity by background light. Another way to study light adaptation is by examining the change in flash sensitivity produced by background light. Fig. 8 depicts one such experiment. The left column shows the cell's responses to the initial turning on of the light steps. At ~ 10 s after the light onset, by which time the step response was already in steady state, flashes were superposed on the light step with an intensity adjusted to elicit a just-detectable response. The timings

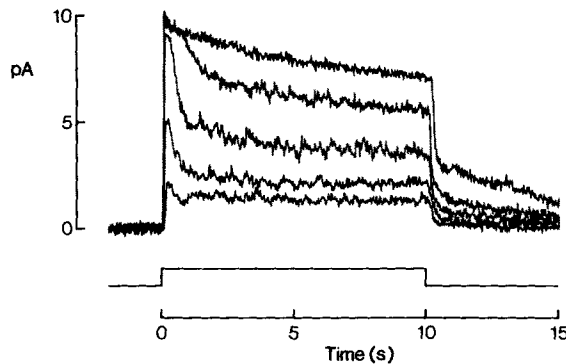


FIGURE 6. Family of responses to light steps from a rabbit rod that shows an unusually high degree of adaptation. Light intensities were 3.5×10^2 , 1.3×10^3 , 5.0×10^3 , 1.8×10^4 , and 7.0×10^4 photons $\mu\text{m}^{-2} \text{s}^{-1}$, respectively; the corresponding responses were averages of 2, 2, 1, 1, and 1 trials. Bandwidth was DC-25 Hz. Temperature was 40°C .

of some of these flashes are indicated by arrowheads on the right column of the figure. Generally, 10–30 flash trials were given at each background intensity. The middle column shows at higher gain the averages of the responses to these incremental flashes. The averaged dim flash response obtained in the absence of background light is shown at the bottom of the figure. It can be noted that there was a progressive shortening of the time-to-peak of the flash response with increasing background intensity, as well as an accelerated recovery of the response. These features are again indications of light adaptation. In this experiment, the time-to-peak of the dim flash response was reduced by $\sim 50\%$ from the situation of no background light to that with the brightest background. In four rods, the average reduction in time-to-peak was $39\% (\pm 9\%, \text{SD})$. This compares to a $\sim 60\%$ reduction in the amphibian rod under similar conditions (from Fig. 14 of Baylor et al., 1980).

The reduction in flash sensitivity as a function of background intensity obtained from the four experiments is shown in Fig. 9 A. The sensitivity reduction is expressed in the normalized form S_F/S_F^D , where S_F is flash sensitivity in the presence of background light and S_F^D is the absolute flash sensitivity without background light

(both in units of picoamperes per photon per square micrometer). The solid curve, which fits the data quite well, is drawn according to:

$$S_F/S_F^D = \frac{1}{1 + I_S/I_O} \quad (4)$$

where I_S is the steady background intensity and I_O is a constant (see Baylor et al., 1980). This is the familiar Weber–Fechner relation, previously shown to apply to the

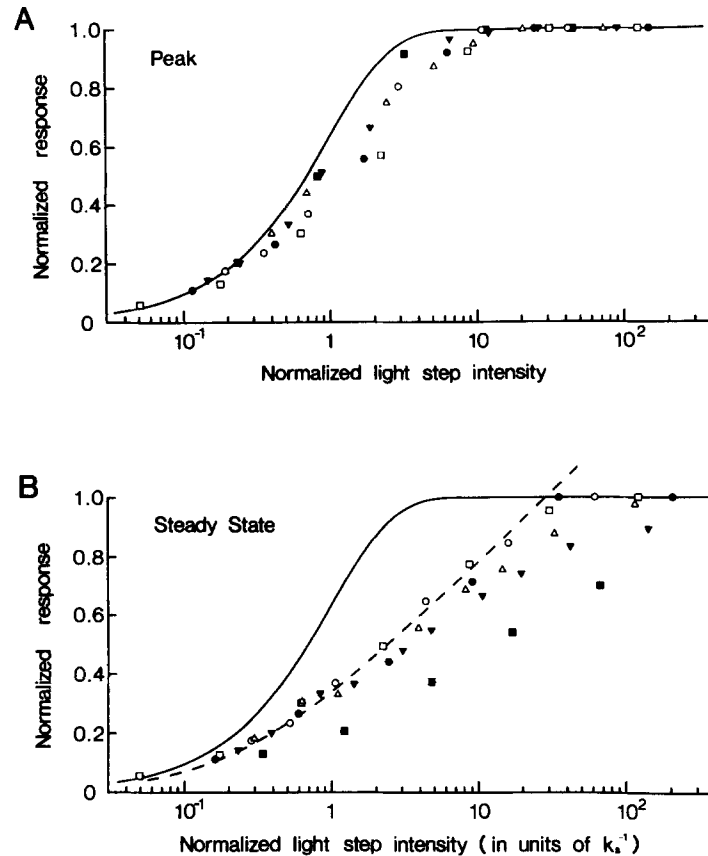


FIGURE 7. Collected step response–intensity relations from six rabbit rods, plotted on normalized axes. (A) Relation at transient peak of responses. (B) Relation at steady state. The unusual cell in Fig. 6 is indicated by the filled square. Continuous curves in both A and B are drawn according to Eq. 3. Dashed curve in B is drawn according to Eq. 7. Temperature range was 38–46°C. Saturated photocurrent was 8–16 pA.

behavior of rods in many lower vertebrates (see Introduction). The value of I_O ranges from 48 to 130 photons $\mu\text{m}^{-2} \text{s}^{-1}$ in the four experiments, with an average of 83 photons $\mu\text{m}^{-2} \text{s}^{-1}$ (or ~ 42 photoisomerizations second $^{-1}$; see Table I). The dashed curve is drawn according to:

$$S_F/S_F^D = e^{-k_S I_S} \quad (5)$$

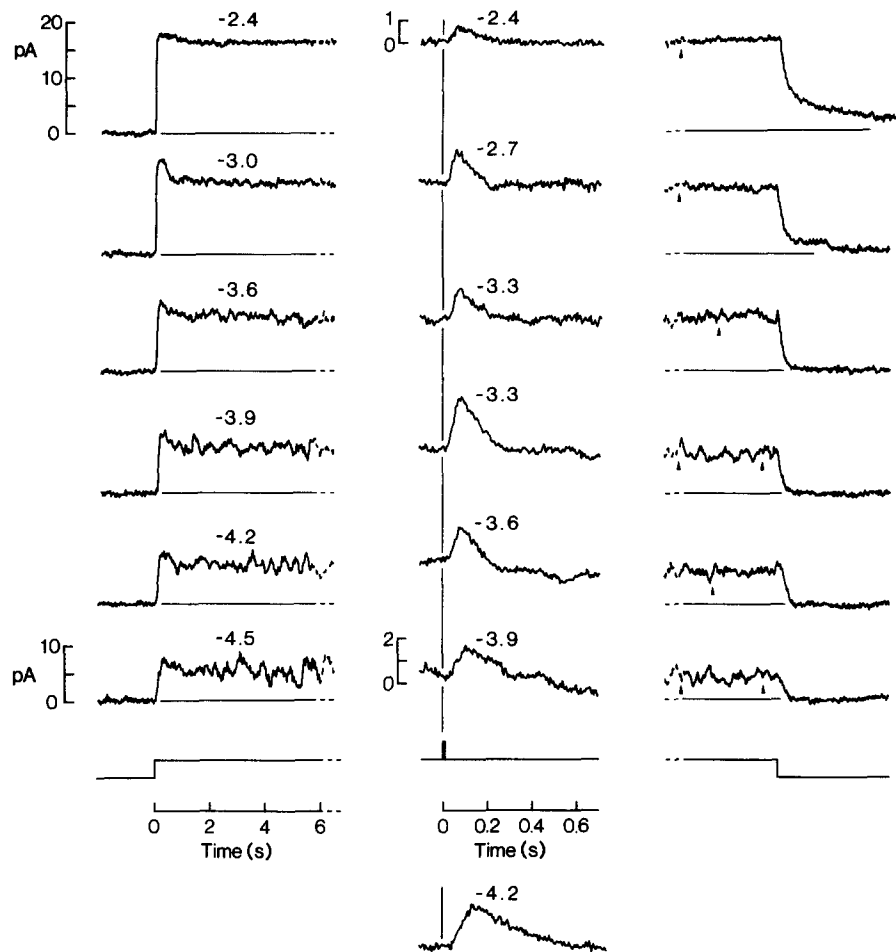


FIGURE 8. Incremental flash response elicited from a rabbit rod in the presence of background light. Left and right columns show the beginning and end of the background light steps and the corresponding responses from the cell. Arrowheads in right column show timings of some flashes superposed on the light steps. Middle column shows, at higher gain, the averaged responses to the incremental flashes at different backgrounds. Flash response at bottom is the control elicited in the absence of background light. The numbers above the traces indicate nominal log attenuations of the light. Actual light step intensities were 1.7×10^2 , 3.5×10^2 , 5.9×10^2 , 1.3×10^3 , 5.0×10^3 , and 1.8×10^4 photons $\mu\text{m}^{-2} \text{s}^{-1}$. Flash intensities were 7.6 (no background), 14, 28, 55, 55, 205, and 409 photons μm^{-2} ; the flash responses were averages of 20, 12, 31, 32, 18, 20, and 21 trials. Bandwidth for left and right columns was DC-25 Hz; that for middle column was DC-100 Hz. Temperature was 40–41°C.

which can be obtained after differentiating Eq. 3 with respect to I_s , and represents the relation expected from the cells' flash sensitivities in darkness if there were no background light adaptation (see Baylor et al., 1984). Overall, the Weber–Fechner relation between incremental flash sensitivity and background intensity was obeyed with sensitivity down to $\sim 1/100$ th of that in darkness. At higher background

intensities the incremental sensitivity began to decline much more rapidly as response saturation was approached.

Flash sensitivity, S_F , can be converted to step sensitivity, S_S , by multiplication with the integration time, t_i , of the flash response (see Baylor and Hodgkin, 1973). Since S_F varies over 100-fold before approaching saturation, whereas the kinetics of the flash response (and hence the integration time) change only slightly by comparison (see above), it is obvious that the change in S_S is dictated by the change in S_F . As

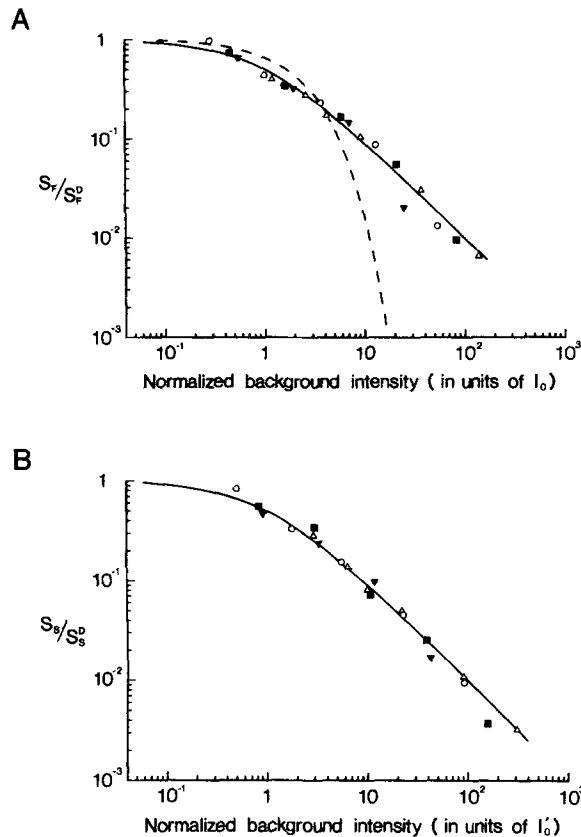


FIGURE 9. Collected results from four incremental flash-on-background experiments on rabbit rods, plotted on normalized axes. (A) Dependence of flash sensitivity on background. Continuous curve is from Eq. 4 and dashed curve is from Eq. 5. The position of the dashed curve relative to the experimental points represents the average position of such curves for all four cells. (B) Dependence of calculated step sensitivity on background. Continuous curve is from Eq. 6. The data obtained from the experiment in Fig. 8 are indicated by the open triangles in both panels. Temperature was 39–41°C. Saturated current was 12–17 pA.

expected, the plot of S_S/S_S^D against background light intensity (Fig. 9 B) can also be described by the Weber–Fechner relation:

$$S_S/S_S^D = \frac{1}{1 + I_S/I'_0} \quad (6)$$

The average I'_0 from the four experiments is 21 photoisomerizations second⁻¹. If the flash response kinetics had remained strictly constant, the values of I_0 and I'_0 would have been identical. The smaller I'_0 reflects a progressive decrease in integration time with increasing background light. Integrating Eq. 6 with respect to I_S , we get:

$$r_s = I'_0 S_S^D \ln(1 + I_S/I'_0) \quad (7)$$

where r_s is the steady-state response to a step of light I_s . The dashed curve in Fig. 7 *B* is drawn according to Eq. 7, using the above I'_0 value and the average S_s^D (normalized against the dark current) from the six experiments; it has been shifted on the abscissa to give the best fit to the collected results. Over most light intensities before saturation, the logarithmic relation describes the experimental data fairly well. This is expected from an internal consistency between the step response–intensity experiments and the incremental–threshold experiments.

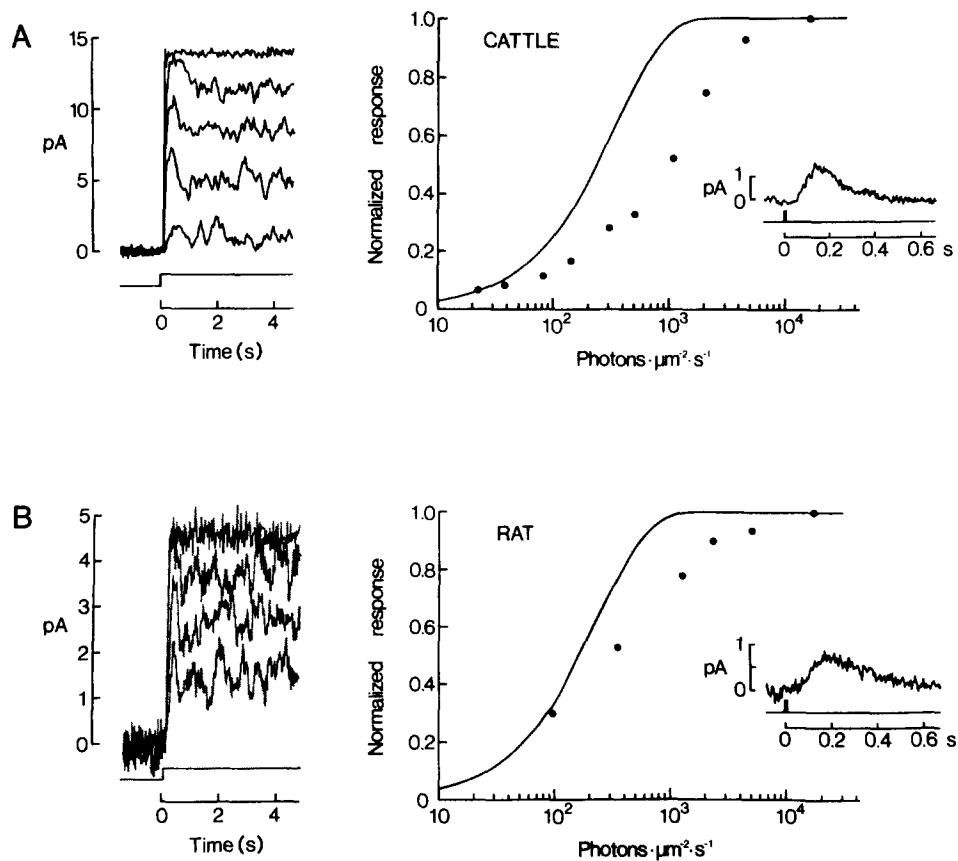


FIGURE 10. (Left) Family of responses to light steps of increasing intensities elicited from a cattle rod (*A*) and a rat rod (*B*). (Right) Normalized response–intensity relations in steady state for the respective experiments. Each step response was normalized with respect to a saturated response elicited by a bright flash immediately before that step response. For each cell, only the responses to a few step intensities are shown on the left because of the large fluctuations, but measurements at all intensities are shown on the right. The responses on the left were averages of (in increasing intensity) 2, 2, 2, 1, and 1 trials in *A* and 2, 2, 1, and 1 trials in *B*. Curves in both *A* and *B* are drawn from Eq. 3. (Insets) Averaged responses of the same cells to dim flashes (in zero background) delivering 6.5 (*A*) and 7.6 (*B*) photons μm^{-2} , respectively. Temperature was 38°C in *A* and 37°C in *B*.

Cattle and Rat

Cattle and rat rods were found to behave in broadly the same way as rabbit rods. Fig. 10 shows sample experiments on these cells using light steps. The smooth curves in the right panels are both drawn from Eq. 3, with positions on the abscissa determined by the size and shape of the respective cell's dim flash response in darkness (insets), according to the relation $k_s = k_F \cdot t_i$ (see above). The maximum photocurrent obtained

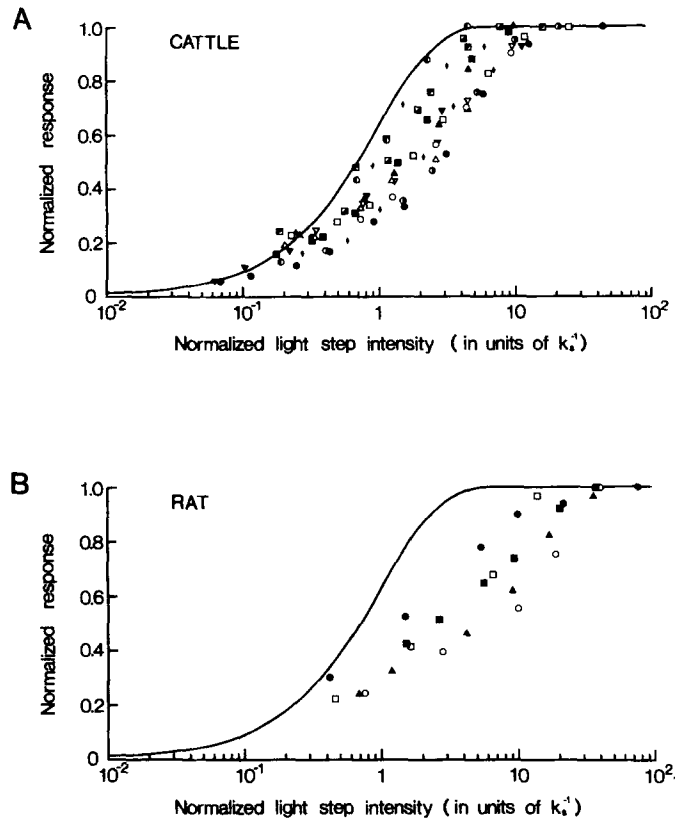


FIGURE 11. Collected step response–intensity relations in steady state from 14 cattle rods and 5 rat rods, plotted on normalized axes. Curves in both *A* and *B* are drawn from Eq. 3 (see text). Saturated photocurrents ranged from 9 to 17 pA in *A* and from 5.4 to 6.3 pA in *B*. Temperature range was 37–41°C in *A* and 36–39°C in *B*.

from rat rods was quite small, most probably because their delicate outer segments were particularly prone to damage; nonetheless, the amplitude of their single-photon responses remained comparable to those in other species (see Table I). The relaxation in the step response of rat rods to light was also less obvious than that seen in rabbit and cattle rods, even though the steady-state response–intensity relation (bottom right panel) indicates a comparable degree of light adaptation. We have previously found the same in cat rods (cf. Figs. 1 and 3 in Tamura et al., 1989). Since

the relaxation reflects how rapidly background adaptation develops with time, this may imply that adaptation takes place more quickly in cat and rat rods than in the other species we have studied. Fig. 11 shows collected steady-state response-intensity relations obtained from both species, giving the same conclusion. Finally, Fig. 12 shows collected results from incremental flash-on-background experiments in the two species. As in rabbit rods, the reduction in flash sensitivity caused by background light was in both cases broadly consistent with the Weber-Fechner relation (solid curve), down to about 1/100th of the sensitivity in darkness. The average value of I_0 was ~ 62 photons $\mu\text{m}^{-2} \text{s}^{-1}$ for cattle rods and ~ 85 photons $\mu\text{m}^{-2} \text{s}^{-1}$ for rat rods.

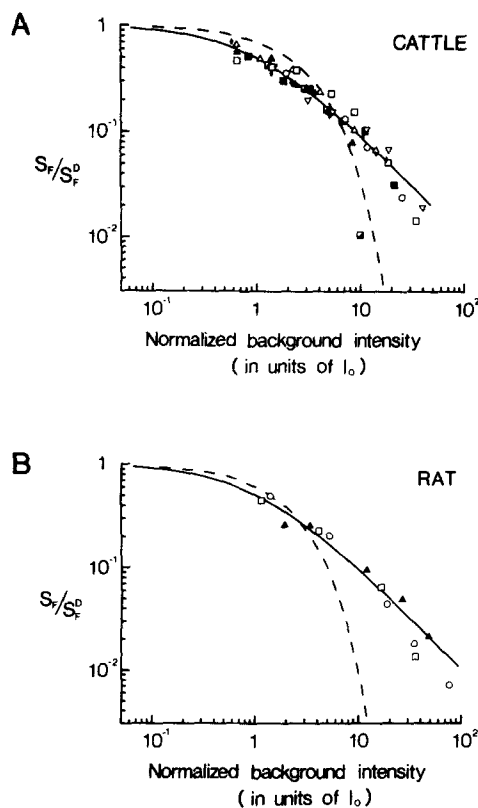


FIGURE 12. Collected results from incremental flash-on-background experiments on nine cattle rods and three rat rods. Continuous curves are from Eq. 4 and dashed curves are from Eq. 5. See Fig. 9 legend. Saturated photocurrent was 9–15 pA in *A* and 5.9–6.2 pA in *B*. Temperature was 37–41°C in *A* and 38–39°C in *B*.

Table I summarizes some measured parameters for the different animal species. The measurements on cat rods from a recent study (Tamura et al., 1989) are also included here for comparison. All light intensities have been converted to approximate numbers of photoisomerizations (Rh^*) for ease of reference.

DISCUSSION

The rods of the several mammals studied here all show the phenomenon of light adaptation. We have recently found the same in cat rods (Tamura et al., 1989). In our

work on cat rods we pointed out that the ability of these cells to adapt to light is quite important, because of a relatively high cone threshold in the cat retina due to the paucity of cones. Thus, without adaptation, the rods in the cat retina would saturate with light before the cones were able to fully take over vision, producing a sensitivity discontinuity in mesopic vision (see Tamura et al., 1989). This should also be true for the rat retina, in which the cone system has a similarly high threshold and does not dominate vision in white light until an intensity producing close to $10^3 \text{ Rh}^* \text{ s}^{-1}$ in individual rods is reached (see Green, 1971; LaVail, 1976). No comparable data are

TABLE I
Collected Parameters for Light Responses of Rods of Different Mammalian Species

Rods	Single-photon response			Steady-state step response		Incremental flash on background
	Peak size	t_p	t_i	Half-saturating I_s	Saturating I_s	I_o
	μA	ms	ms	$Rh^* \text{ s}^{-1}$	$Rh^* \text{ s}^{-1}$	$Rh^* \text{ s}^{-1}$
Rabbit	0.81 ± 0.44 (7)* [†]	161 ± 17 (7) [†]	376 ± 74 (7) [†]	245 ± 51 (5) [†]	$\sim 6,000$ (5) [†]	42 ± 16 (4)
Cattle	0.57 ± 0.24 (14)*	219 ± 29 (14)	295 ± 70 (14)	180 ± 90 (14)	$\sim 4,000$ (14) [†]	31 ± 20 (9)
Rat	0.54 ± 0.39 (6)*	238 ± 82 (6)	333 ± 105 (6)	161 ± 77 (5)	$\sim 4,000$ (5) [†]	30 ± 15 (3)
Cat [‡]	1.12 ± 0.30 (8)*	154 ± 16 (8)	263 ± 69 (8)	179 ± 109 (7)	$\sim 4,000$ (7) [†]	35 ± 11 (4)

Each entry shows the mean and the standard deviation; the number in parentheses indicates the number of cells studied. t_p , time-to-peak; t_i , integration time; I_s , steady light intensity; I_o , constant in the Weber–Fechner relation (Eq. 4); Rh^* , rhodospin photoisomerizations. The numbers in Rh^* were calculated from calibrated light intensities and an effective collecting area (transverse light incidence, unpolarized) of $0.5 \mu\text{m}^2$ for rabbit and cattle rods and $0.35 \mu\text{m}^2$ for cat and rat rods. These effective collecting areas were in turn calculated by assuming that completely intact rod outer segments from these mammalian species would have a length of $25 \mu\text{m}$.

*These single-photon response amplitudes were estimated from the ratio σ^2/m (see text). Separate calculations based on light calibrations and individual cells' effective collecting areas gave estimates that were within a factor of 2 from these values.

[†]In calculating these averages, the rabbit rod in Fig. 6 has been excluded because its behavior was rather extreme.

[‡]These numbers are only rough values because of an asymptotic approach to saturation by the light responses.

[§]Data taken from Tamura et al. (1989).

available for rabbit and cattle, though circumstantial observations (see Elenius, 1958; Hughes, 1971) may suggest a similar situation, at least in the rabbit.

Previously, Penn and Hagins (1972) have studied rat rods using mass extracellular recordings, but their conclusion was puzzling. They found that flash sensitivity was reduced by background light according to the Weber–Fechner (or inverse) relation (i.e., similar to what we have reported here [Eq. 4]), but concluded that this was sufficiently accounted for by simple compression of the flash response amplitude at high light intensities according to the Michaelis (or hyperbolic) relation. We believe this is incorrect. Strict hyperbolic compression predicts a flash sensitivity that decreases inversely as the *square*, rather than the first power, of background in-

tensity (see also Adelson, 1982). This can be realized by differentiating the relation $\hat{r}_s = I_s / (I_s + \sigma_s)$ with respect to I_s , which gives the step sensitivity $S_s \equiv d\hat{r}_s / dI_s \propto (I_s + \sigma_s)^{-2}$. With the flash sensitivity $S_f \propto S_s$, we get $S_f \propto (I_s + \sigma_s)^{-2}$.

It could have appeared that one way of deriving the desired inverse relation from the hyperbolic relation, $\hat{r}_s = I_s / (I_s + \sigma_s)$, would be to consider the variable $\tilde{r}_s \equiv 1 - \hat{r}_s = \sigma_s / (I_s + \sigma_s)$, which represents the residual dynamic range for the light response in the presence of background I_s . By arguing that the incremental flash sensitivity, S_f , on background should be directly proportional to \tilde{r}_s , it would then have appeared that $S_f \propto (I_s + \sigma_s)^{-1}$. This derivation implied that I_0 was equal to σ_s , or to σ_f / t_i , where t_i is the integration time of the flash response (assuming constant response kinetics). Indeed, Penn and Hagins (1972) appeared to have equated I_0 with σ_s (see their p. 1083). This line of reasoning, however, is incorrect, because background light not only reduces the residual dynamic range, but also translates the position of the cell some distance up the hyperbolic relation; as a result, the residual dynamic range is governed by a new hyperbolic relation with σ_s replaced by $I_s + \sigma_s$ (this can be arrived at with some simple algebra). Incorporating this feature gives $S_f \propto (I_s + \sigma_s)^{-2}$, the same reciprocal square relation as in the previous paragraph.

While strict hyperbolic compression does not directly lead to the Weber–Fechner type of desensitization, it is worth emphasizing that the hyperbolic relation itself reflects the presence of light adaptation. When adaptation is negligible or absent, the intensity–response relation for a rod is described by the steeper exponential function, and not the hyperbolic function. This is the case, for example, at early times after a flash (see first section of Results here, and Lamb et al., 1981), or when the calcium feedback mediating adaptation is mostly removed experimentally (Matthews et al., 1988; Nakatani and Yau, 1988a).

We find that the value of I_0 , which is the constant in the Weber–Fechner relation (Eq. 4) and sometimes referred to as the “dark light,” does not vary much among the different mammalian species, ranging from 30 to 40 photoisomerizations (Rh^*) s^{-1} (see Table I). A roughly similar value can be derived from Steinberg’s (1971) incremental threshold experiments on retinal pigment epithelial cells of the cat, which indirectly reflect rod activity. On the other hand, Penn and Hagins (1972) found that it took an average of 350 photons absorbed per rod per second, or $\sim 235 \text{ Rh}^* \text{ rod}^{-1} \text{ s}^{-1}$ (assuming a quantum efficiency of 0.67), to reduce the rat rod’s sensitivity by half. This discrepancy by almost a factor of 10 between their number and ours is disturbing. Indeed, the large number reported by Penn and Hagins (1972) also seems inappropriately high when considered with other information in their paper. Thus, they reported that each absorbed photon produced a peak response equal to $\sim 3\%$ of maximum in a rat rod. From their Fig. 2, the integration time of the dim flash response was 0.3–0.4 s at 33–36°C (which is close to what we report here for the same species; see Table I). Thus, a steady background light producing 1 absorbed photon $\text{rod}^{-1} \text{ s}^{-1}$ should give a mean response equal to $\sim 0.03 \times 0.35 \approx 0.01$ of maximum. At this rate, it is very difficult to see how the incremental flash sensitivity could still be constant up to 100 absorbed photons $\text{rod}^{-1} \text{ s}^{-1}$, as they found (see their Fig. 6).

In cold-blooded vertebrates, the value of I_0 seems much more variable, being $\sim 0.2 \text{ Rh}^* \text{ s}^{-1}$ in turtle (Copenhagen and Green, 1985), 4–10 $\text{Rh}^* \text{ s}^{-1}$ in tropical toad (Fain,

1976; Baylor et al., 1980; Lamb et al., 1981), and $\sim 30 \text{ Rh}^* \text{ s}^{-1}$ in larval tiger salamander (Matthews et al., 1988, and our unpublished observation). On the whole, these I_0 values are lower than in mammalian species. This difference is expected, however, because even though the amplitude of the single-photon response is not very different between cold- and warm-blooded animals, the integration time of the response is considerably longer in cold-blooded animals (mostly because of the lower temperature). Thus, it should take a dimmer light to produce the same degree of steady excitation in toads rods than in, for example, rabbit rods (compare Fig. 1 in

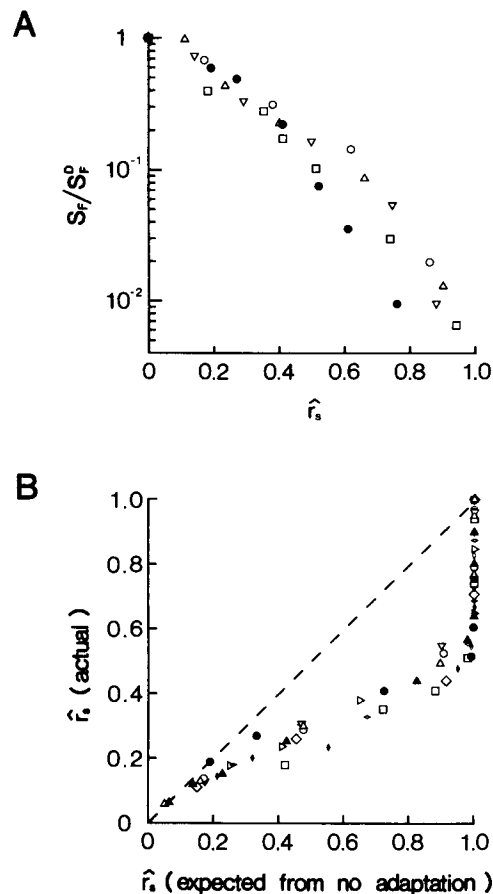


FIGURE 13. Comparison between background adaptations in rabbit and toad rods (and a salamander rod). (A) Log-linear plot of incremental flash sensitivity against the steady response to background light; both normalized. *Open symbols*, data from the four rabbit rods in Fig. 9; *filled circles*, measurements from the toad rod in Figs. 14 and 15 of Baylor et al. (1980). (B) Actual steady response to a step of light plotted against the expected response if adaptation were absent; both normalized. Dashed line indicates the expected relation without adaptation. *Open symbols*, combined data from the rabbit rods in Fig. 9 and those in Fig. 7 (the unusual cell marked by the filled squares in Fig. 7 is omitted; also, one cell was common to both Figs. 7 and 9). *Filled circles*, same toad rod as in A; *filled triangles*, measurements from the tiger salamander rod in Fig. 1A of Nakatani and Yau (1988a).

Baylor et al., 1979b with Fig. 4 here; see also Fain, 1976; Lamb, 1986). The same should therefore be true for light adaptation, which arises as a negative feedback from the excitation (see references in Introduction). To examine this point more closely, we have compared, as an example, the adaptation measurements from rabbit and toad rods, shown in Fig. 13. In A, S_F/S_F^D is plotted against \hat{r}_s (the normalized steady response to background light), so that we are examining, roughly, how the degree of adaptation depends on the steady degree of excitation in the two species. The rabbit rods (open symbols) are from the collected results of Fig. 9A here, while

the toad rod (filled circles) is from Figs. 14 and 15 of Baylor et al. (1980). It is clear from Fig. 13 *A* that the relations between S_F/S_F^D and \hat{r}_s from the two species overlap reasonably well, despite a much higher I_O for rabbit rods (ranging 24–65 $\text{Rh}^* \text{s}^{-1}$, with a mean of 42 $\text{Rh}^* \text{s}^{-1}$; see Table I) than for the toad rod (5–10 $\text{Rh}^* \text{s}^{-1}$; see Baylor et al., 1980). In both cases the incremental flash sensitivity decreases by a factor of two when the steady response to background reaches about one-fourth of maximum. Fig. 13 *A* is easy to understand, but it has the drawback that \hat{r}_s is not exactly an independent variable, being itself dependent on the degree of adaptation present. A more appropriate comparison of adaptation in rabbit and toad rods is to plot the *measured* \hat{r}_s at different light step intensities against the corresponding *expected* \hat{r}_s if adaptation were absent (the latter can be obtained from the exponential curve in plots like those in Fig. 7 *B*). Plotting the measured \hat{r}_s on the ordinate also has the advantage that adaptational changes in response amplitude and kinetics can be considered together because \hat{r}_s depends on the multiplicative product of response amplitude and integration time. In Fig. 13 *B*, the rabbit and toad rods (see figure legend) are compared in this manner, revealing again the quantitative similarity between the two species. For a broader comparison across species, we have also included in this latter plot the measurements from a tiger salamander rod (filled triangles) in our previous work (Nakatani and Yau, 1988*a*), which leads to the same conclusion. Thus, there does not appear to be any significant difference between mammals and lower vertebrates in the “gain” of the process leading from excitation to adaptation in rods. In contrast, the more severe adaptation in cones than in rods is obvious even in the same species (see, for example, Figs. 2 *A* and 4 *A* of Nakatani and Yau, 1988*a*, for a comparison between salamander rods and cones).

The difference in body temperature probably also explains the different rates of relaxation of the step responses in amphibian and mammalian rods. In amphibian rods, this relaxation (at $\sim 20^\circ\text{C}$) is largely complete in 5–10 s after the onset of light (see, for example, Baylor et al., 1980; Nakatani and Yau, 1988*a*). In rabbit and cattle rods, on the other hand, the relaxation (at 38–40°C) takes only 1–2 s to complete after light onset (see Figs. 4, 6, 8, and 10 here); the relaxation rates in rat and cat rods are probably comparable, or perhaps even faster (see Results). Part of this difference in speed between cold- and warm-blooded vertebrates may reflect the temperature sensitivity of the Na^+ - Ca^{2+} exchange, which pumps down free Ca^{2+} in the rod outer segment during illumination to bring about the Ca^{2+} -mediated negative feedback underlying background adaptation (Yau and Nakatani, 1985; McNaughton et al., 1986; Nakatani and Yau, 1988*b*; Ratto et al., 1988). In four experiments of studying rabbit rods at room temperature (22–24°C), we found that the relaxation of the step response took close to 5 s to complete (data not shown), rather similar to that shown by amphibian rods at the same temperature.

In addition to cat rods and those of the several mammals described in this paper, we have now also examined rods from several primate species, with essentially the same finding (Tamura, T., K. Nakatani, and K.-W. Yau, manuscript submitted for publication). Re-examining the previous work of Baylor et al. (1984) on macaque rods, we found that at least two of the seven cells in their collected results (their Fig. 9) showed desensitization that was better fitted by the Weber–Fechner relation than the exponential function for zero adaptation. Thus, light adaptation is likely to be a

universal property among all vertebrate rods. The salamander *Necturus* is somewhat unique among the cold-blooded vertebrates that have been studied, in that it is the only species whose rods apparently show little light adaptation (Norman and Werblin, 1974). In light of our present findings, however, a reexamination of these cells may be worthwhile.

We thank Dr. S. Kaushal for participating in a few of the experiments, and Drs. W. B. Guggino, R. E. Mains, and S. H. Snyder for providing some of the animals. Dr. R. E. Marc of the University of Texas Medical Center at Houston has kindly measured for us the lengths of some rabbit rod outer segments from his fixed retinal specimens. Finally, we thank Drs. D. A. Baylor, N. W. Daw, L. W. Haynes, R. H. Masland, B. Minke, J. Nathans, R. F. Nelson, J. L. Schnapf, R. M. Shapley, and S. M. S. Wu for discussions. One of the reviewers of this paper has kindly suggested adding Fig. 9 B, as well as inserting the dashed curve in Fig. 7 B based on Eq. 7.

This work was supported by a grant from the U. S. National Eye Institute.

Original version received 20 March 1990 and accepted version received 18 July 1990.

REFERENCES

- Adelson, E. H. 1982. Saturation and adaptation in the rod system. *Vision Research*. 22:1299–1312.
- Baylor, D. A., and A. L. Hodgkin. 1973. Detection and resolution of visual stimuli by turtle photoreceptors. *Journal of Physiology*. 234:163–198.
- Baylor, D. A., and A. L. Hodgkin. 1974. Changes in time scale and sensitivity in turtle photoreceptors. *Journal of Physiology*. 242:729–758.
- Baylor, D. A., T. D. Lamb, and K.-W. Yau. 1979a. The membrane current of single rod outer segments. *Journal of Physiology*. 288:589–611.
- Baylor, D. A., T. D. Lamb, and K.-W. Yau. 1979b. Responses of retinal rods to single photons. *Journal of Physiology*. 288:613–634.
- Baylor, D. A., G. Matthews, and B. J. Nunn. 1984. Location and function of voltage-sensitive conductances in retinal rods of the salamander, *Ambystoma tigrinum*. *Journal of Physiology*. 354:203–223.
- Baylor, D. A., G. Matthews, and K.-W. Yau. 1980. Two components of electrical dark noise in toad retinal rod outer segments. *Journal of Physiology*. 309:591–621.
- Baylor, D. A., and B. J. Nunn. 1986. Electrical properties of the light-sensitive conductance of rods of the salamander *Ambystoma tigrinum*. *Journal of Physiology*. 371:115–145.
- Baylor, D. A., B. J. Nunn, and J. L. Schnapf. 1984. The photocurrent, noise and spectral sensitivity of rods of the monkey *Macaca fascicularis*. *Journal of Physiology*. 357:575–607.
- Coles, J. A., and S. Yamane. 1975. Effects of adapting lights on the time course of the receptor potential of the anuran retinal rod. *Journal of Physiology*. 247:189–207.
- Copenhagen, D. R., and D. G. Green. 1985. The absence of spread of adaptation between rod photoreceptors in turtle retina. *Journal of Physiology*. 369:161–181.
- Dartnall, H. J. A. 1972. Photosensitivity. In *Photochemistry of Vision*. H. J. A. Dartnall, editor. Springer Verlag, New York. 122–145.
- Dowling, J. E., and H. Ripps. 1972. Adaptation in skate photoreceptors. *Journal of General Physiology*. 60:698–719.
- Elenius, V. 1958. Recovery in the dark of the rabbit's electroretinogram in relation to intensity, duration and colour of light-adaptation. *Acta Physiologica Scandinavica*. 44 (Suppl. 150):5–57.
- Fain, G. L. 1976. Sensitivity of toad rods: dependence on wavelength and background illumination. *Journal of Physiology*. 261:71–101.

- Gold, G. H. 1986. Plasma membrane calcium fluxes in intact rods are inconsistent with the calcium hypothesis. *Proceedings of the National Academy of Sciences USA* 83:1150–1154.
- Green, D. G. 1971. Light adaptation in the rat retina: evidence for two receptor mechanisms. *Science*. 174:598–600.
- Harosi, F. I. 1975. Absorption spectra and linear dichroism of some amphibian photoreceptors. *Journal of General Physiology*. 66:357–382.
- Hemilä, S. 1977. Background adaptation in the rods of the frog's retina. *Journal of Physiology*. 265:721–741.
- Hodgkin, A. L., P. A. McNaughton, B. J. Nunn, and K.-W. Yau. 1984. Effect of ions on retinal rods from *Bufo marinus*. *Journal of Physiology*. 350:649–680.
- Hodgkin, A. L., and B. J. Nunn. 1988. Control of light-sensitive current in salamander rods. *Journal of Physiology*. 403:439–471.
- Hughes, A. 1971. Topographical relationships between the anatomy and physiology of the rabbit visual system. *Documenta Ophthalmologica*. 30:33–159.
- Kawamura, S., and M. Murakami. 1989. Regulation of cGMP levels by guanylate cyclase in truncated frog rod outer segments. *Journal of General Physiology*. 94:649–668.
- Kleinschmidt, J., and J. E. Dowling. 1975. Intracellular recordings from *Gecko* photoreceptors during light and dark adaptation. *Journal of General Physiology*. 66:617–648.
- Koch, K.-W., and L. Stryer. 1988. Highly cooperative feedback control of retinal rod guanylate cyclase by calcium ions. *Nature*. 334:64–66.
- Korenbrod, J. I., and D. L. Miller. 1986. Calcium ions act as modulator of intracellular information flow in retinal rod phototransduction. *Neuroscience Research*. Suppl. 4:S11–S34.
- Lamb, T. D. 1986. Photoreceptor adaptation: vertebrates. In *The Molecular Mechanism of Photoreception*. Dahlem Konferenzen. H. Stieve, editor, Springer Verlag, Berlin. 267–286.
- Lamb, T. D., P. A. McNaughton, and K.-W. Yau. 1981. Spatial spread of activation and background desensitization in toad rod outer segments. *Journal of Physiology*. 319:463–486.
- LaVail, M. M. 1976. Survival of some photoreceptor cells in albino rats following long-term exposure to continuous light. *Investigative Ophthalmology and Visual Science*. 15:64–70.
- Leibovic, K. N., J. E. Dowling, and Y. Y. Kim. 1987. Background and bleaching equivalence in steady-state adaptation of vertebrate rods. *Journal of Neuroscience*. 7:1056–1063.
- Liebman, P. A. 1972. Microspectrophotometry of photoreceptors. In *Photochemistry of Vision*. H. J. A. Dartnall, editor. Springer Verlag, New York. 481–528.
- Matthews, H. R., R. L. W. Murphy, G. L. Fain, and T. D. Lamb. 1988. Photoreceptor light adaptation is mediated by cytoplasmic calcium concentration. *Nature*. 334:67–69.
- McNaughton, P. A., L. Cervetto, and B. J. Nunn. 1986. Measurement of the intracellular free calcium concentration in salamander rods. *Nature*. 322: 261–263.
- Miller, D. L., and J. I. Korenbrot. 1987. Kinetics of light-dependent Ca fluxes across the plasma membrane of rod outer segments. A dynamic model of the regeneration of cytoplasmic Ca concentration. *Journal of General Physiology*. 90:397–426.
- Nakatani, K., and K.-W. Yau. 1988a. Calcium and light adaptation in retinal rods and cones. *Nature*. 334:69–71.
- Nakatani, K., and K.-W. Yau. 1988b. Calcium and magnesium fluxes across the plasma membrane of the toad rod outer segment. *Journal of Physiology*. 395:695–729.
- Nakatani, K., and K.-W. Yau. 1989a. Light adaptation in retinal rods of the rabbit. *Biophysical Journal*. 55:63a. (Abstr.)
- Nakatani, K., and K.-W. Yau. 1989b. Sodium-dependent calcium extrusion and sensitivity regulation in retinal cones of the salamander. *Journal of Physiology*. 409:525–548.

- Normann, R. A., and F. S. Werblin. 1974. Control of retinal sensitivity. I. Light and dark adaptation of vertebrate rods and cones. *Journal of General Physiology*. 63:37–61.
- Penn, R. D., and W. A. Hagins. 1972. Kinetics of the photocurrent of retinal rods. *Biophysical Journal*. 12:1073–1094.
- Pugh, E. N., and J. Altman. 1988. A role for calcium in adaptation. *Nature*. 334:16–17.
- Ratto, G. M., R. Payne, W. G. Owen, and R. Y. Tsien. 1988. The concentration of cytosolic free calcium in vertebrate rod outer segments measured with Fura-2. *Journal of Neuroscience*. 8:3240–3246.
- Rispoli, G., W. A. Sather, and P. B. Detwiler. 1988. Effect of triphosphate nucleotides on the response of detached rod outer segments to low external calcium. *Biophysical Journal*. 53:338a. (Abstr.)
- Shapley, R., and C. Enroth-Cugell. 1984. Visual adaptation and retinal gain controls. *Progress in Retinal Research*. 3:263–346.
- Steinberg, R. H. 1971. Incremental responses to light recorded from pigment epithelial cells and horizontal cells of the cat retina. *Journal of Physiology*. 217:93–110.
- Tamura, T., K. Nakatani, and K.-W. Yau. 1989. Light adaptation in cat retinal rods. *Science*. 245:755–758.
- Torre, V., H. R. Matthews, and T. D. Lamb. 1986. Role of calcium in regulating the cyclic GMP cascade of phototransduction in retinal rods. *Proceedings of the National Academy of Sciences USA*. 83:7109–7113.
- Yau, K.-W., and D.A. Baylor. 1989. Cyclic GMP-activated conductance of retinal photoreceptor cells. *Annual Review in Neuroscience*. 12:289–327.
- Yau, K.-W., L.W. Haynes, and K. Nakatani. 1986. Roles of calcium and cyclic GMP in visual transduction. In *Membrane Control of Cellular Activity*. H. Ch. Lüttgau, editor. Gustav Fischer Verlag GmbH & Co. KG, Stuttgart. 343–366.
- Yau, K.-W., and K. Nakatani. 1985. Light-induced reduction of cytoplasmic free calcium in retinal rod outer segment. *Nature*. 313:579–582.